Impact Dynamics of Large Dimensional Systems

M. E. Homer*and S. J. Hogan†

Department of Engineering Mathematics

University of Bristol

Bristol BS8 1TR

United Kingdom

February 3, 2006

Abstract

In this paper we present a model of impact dynamics in large dimensional systems. We describe a hybrid method, based on graph theory and probability theory, which enables us qualitatively to model the statistics of global dynamics as parameters are varied. Direct numerical simulation reveals a sudden jump from no impacts within the system to many repeated impacts at a critical value of system parameters. We show that a simple model of the most likely number of impacts also possesses a sudden jump and gives good agreement with the numerical results for large impact probability. A refinement of this model improves the agreement at lower impact probability values.

1 Introduction

We consider a large dimensional *piecewise smooth* (PWS) dynamical system. PWS systems may be described by equations of the form

$$\dot{x} = f(x, t, \mu), \tag{1}$$

*martin.homer@bristol.ac.uk

†s.j.hogan@bristol.ac.uk

where $f : \mathbb{R}^{m+p+1} \to \mathbb{R}^m$ is a piecewise smooth function, $\mu \in \mathbb{R}^p$ is a vector of parameters and $x \in \mathbb{R}^m$. Low dimensional (small m) versions of such systems have extremely rich dynamics. They occur in a variety of physical systems in engineering and applied science. Examples include systems with impacts [Thompson & Ghaffari, 1982; Goyder & Teh, 1989; Budd & Dux, 1994; Holmes, 1982], as well as systems in power electronics [di Bernardo *et al.*, 1998], geared systems [Halse *et al.*, 2006], earthquake engineering [Hogan, 1995], and structural engineering [Doole & Hogan, 1996; Lazer & McKenna, 1990]. Much recent research has concentrated on bifurcations unique to such systems (see Kowalczyk *et al.* [2006], and references therein). Large dimensional piecewise smooth systems, however, are much less well understood.

We consider the following model problem in which n masses oscillate parallel to the x-axis, confined between two side walls (see Fig. 1). The equilibrium positions of the masses are uniformly spread at a distance d apart along this axis. The masses can impact nearest neighbours only. Between impacts, the motion of each mass is governed by the differential equation

$$m_j \frac{\mathrm{d}^2 x_j}{\mathrm{d}t^2} + \omega_j^2 (x_j - jd) = F_j(t), \tag{2}$$

where m_j is the jth mass at position $x_j(t)$ and ω_j is its natural frequency. The forcing $F_j(t)$ is assumed to be of the form

$$F_j(t) = \sum_{i=1}^{\infty} \alpha_{i,j} \cos \Omega_i t + \beta_{i,j} \sin \Omega_i t, \tag{3}$$

where $\alpha_{i,j}$ and $\beta_{i,j}$ are independent random variables and Ω_i are a set of forcing frequencies; we use this, as in Rice [1945], as a simple model of random forcing. Damping is provided by impacts between masses through the Newtonian coefficient of restitution.

This model is related to that of Toda [1989], where an exponential force was assumed between masses in a single row of oscillators. Under harmonic forcing, the system in [Toda, 1989] was shown to possess complex dynamics [Geist & Lauterborn, 1988], and when viscous damping and spring stiffness were added, a sensitivity to initial conditions was observed [Davies & Moon, 1994]. In a related problem [Kuroda & Moon, 2001], an experiment was described in which a periodic array of elastic oscillators was placed in a steady cross flow. At a critical value of the flow speed, the oscillators appear to exhibit chaotic dynamics. Such threshold phenomena are known to occur in heat exchangers [Goyder & Teh, 1989; Kim & Jung, 2000] and are thought to be responsible for

reduced operational lifetime in these critical components of the nuclear industry.

Our approach is to investigate the statistics of impacts in Eqs. (2) and (3) as the forcing amplitude is increased, first via numerical simulation and then by analytic methods.

2 Numerical Simulations

We choose a scaling such that $d = 1, m_j = 1, \omega_j = 1$, so Eq. (2) becomes

$$\frac{\mathrm{d}^2 x_j}{\mathrm{d}t^2} + (x_j - j) = F_j(t), \tag{4}$$

and we take $F_j(t)$ to have just one component

$$F_j(t) = \alpha_{1,j} \cos \Omega t + \beta_{1,j} \sin \Omega t, \tag{5}$$

where $\alpha_{1,j}$ and $\beta_{1,j}$ are identically distributed independent normal random variables, with zero mean and variance σ^2. We set $\Omega = \sqrt{2}$, and assume a coefficient of restitution $r = 0.8$ at impact. We simulate the system of Eqs. (4) and (5) with 100 masses (taking the two end walls to be indistinguishable from the masses), and record the number of impacts after a suitable transient time has elapsed. Solutions which have no impacts after the transient are discarded (for further details see Homer [1999]). Figures 2 and 3 respectively show plots of the most likely number and the expected number of impacts as a function of σ. For this range of parameter values, the number of three-way impacts is negligible, as is the incidence of sticking; these are important observations for the analysis later in the paper. Figures 2 and 3 show that for small σ there are very few impacts, but as σ is increased past a threshold ($\sigma \approx 0.12$) the number of impacts increases very rapidly. Such a threshold is clearly present in the case of two masses (where a low enough force means that the masses can never hit each other), but it is perhaps surprising that a large dimensional system exhibits this behaviour, which is reminiscent of percolation theory [Stauffer, 1985]. We now seek an explanation for this jump.

3 PWS Systems and Graph Theory

We recall that in previous work [Hogan & Homer, 1999; Homer, 1999] we demonstrated how graph theory [Biggs *et al.*, 1976] may be used to find periodic orbits in general PWS dynamical systems. The key idea is to represent the system as a directed graph. Specifically the relationship between the PWS of this paper and a graph can be summarised as follows:

- impacts are interpreted as vertices of a directed graph of the system,
- the evolution of the system between two impacts is an edge of the graph between the two corresponding vertices, and
- the direction along an edge corresponds to increasing time.

Every periodic orbit in the dynamical system can be represented as a circuit in the graph, every one of which can be found algorithmically; see Hogan & Homer [1999] for full details.

We now describe a graph representing our model. With n masses, there are $n+1$ possible impacts; namely $n-1$ mass-mass impacts, and 2 mass-wall impacts. In Fig. 4 we have $n=3$, so there are 4 vertices in the graph (corresponding to 2 mass-mass impacts and 2 mass-wall impacts). The 16 edges correspond to all the possible evolutions of the system between the vertices. A particular periodic orbit in the system involves some of the vertices and some of the edges. In fact different circuits in this graph correspond to different periodic orbits in the dynamical system. For example the circuit shown in Fig. 5(a) has its equivalent physical evolution shown in Fig. 5(b). Similarly the circuit shown in Fig. 6(a) has its equivalent physical evolution shown in Fig. 6(b).

4 Periodic Orbits

We now make the fundamental assumption that the response of the system to an external forcing, that is Figs. 2 and 3, consists of a mixture of different periodic orbits that go to make up a fully connected graph, as illustrated in Fig. 4. For low values of σ, the orbits that make up the system response will have few impacts each and for large values of σ the orbits will have many impacts each.

So, as a function of σ, we need some idea of the distribution of types of orbit and some way of

deciding how often each different type of orbit occurs. Using graph theory it is straightforward to count and classify these orbits. We shall begin this calculation in Sec. 5. The problem of deciding how likely any particular orbit is to occur is more difficult. In essence it requires a knowledge of the relative size of the basin of attraction of each orbit, for given parameter values. A simpler method is to argue that a graph edge occurs with probability $p \in [0, 1]$. In this way an orbit (circuit of the graph) with k trajectory segments (k edges) occurs with probability proportional to p^k. We incorporate probability into our analysis in Sec. 6.

5 Distribution of Orbits

To count the different types of orbit, we divide the circuits into classes. We first consider simple circuits, where no vertex in the graph is visited more than once (it is not necessary to visit every vertex). In physical terms, simple circuits of length k correspond to periodic orbits, with $k + 1$ masses undergoing a sequence of impacts with no repeats. So, for example, in the simple circuit in Fig. 5 the left hand wall and the first mass collide, then the first and second mass collide, followed by the third mass and the right hand wall. So the sequence of impacts here is L-1, 1-2, 3-R. Contrast this with the sequence for the non-simple orbit in Fig. 6 which is L-1, L-1, 1-2, L-1, 2-3, 1-2, 3-R, 3-R where the L-1 impact is repeated twice and the 1-2 and 3-R impacts repeated once each. We shall return to the subject of non-simple circuits in Sec. 9.

In a fully connected graph with N vertices, the number of distinct paths of length k with the same initial and final vertex is

$$(N-1)(N-2)\dots(N-(k-1)) = \frac{(N-1)!}{(N-k)!}, \tag{6}$$

because, in order to complete a valid path, we must choose $k-1$ additional vertices, all different. Thus the number of distinct simple circuits of length $k \in \{1, \dots, N\}$ in a graph with N vertices, $\phi_N(k)$, is given by

$$\phi_N(k) = \frac{N!}{k(N-k)!}, \tag{7}$$

since there are N choices of the initial vertex i, with each circuit repeated k times (once for each vertex along its length).

If N is large, the ratio

$$\frac{\phi_N(k)}{\phi_N(N)} = \frac{N}{k(N-k)!} \ll 1 \tag{8}$$

for all $k \lessapprox N$. Thus the majority of simple circuits have length $\approx N$, the size of the whole system. In physical terms, most of the periodic orbits involving a sequence of impacts with no repeats are the size of the whole system. This effect is demonstrated in Fig. 7.

6 Probability

We now address the problem of deciding how likely a circuit (orbit) of length k is to occur. As mentioned in Sec. 4, we associate a weight $p_{ij} \in [0,1]$ with each edge of the graph between neighbouring vertices i and j. For simplicity, we will assume that the p_{ij} are all equal to some constant value p. We also assume that impacts occur independently.

Therefore the probability of a simple circuit of length k is proportional to $p^k\phi_N(k)$. We take the sample space to be all possible simple circuits. In other words, all possible simple circuits are included and no non-simple circuits are included. We shall discuss the relaxation of both these assumptions in Secs. 8 and 9. Thus if X is the number of different mass-mass impacts, it has the distribution

$$P(X=k) = \frac{p^k\phi_N(k)}{\sum_{j=1}^{N} p^j\phi_N(j)} = \frac{\Phi_{N,p}(k)}{\Gamma_{N,p}}, \tag{9}$$

where

$$\Phi_{N,p}(k) = \frac{p^k N!}{k(N-k)!}, \qquad \Gamma_{N,p} = \sum_{j=1}^{N} \frac{p^j N!}{j(N-j)!} \tag{10}$$

(so that $\sum_{k=1}^{N} P(X=k) = 1$).

Figure 8 shows $P(X=k)$ for various values of the parameter p. For small values of p we expect to see very few impacts (Fig. 8(a)), while for very small increase in p the number of impacts increases rapidly towards the size of the whole system, where each mass undergoes an impact (Figs. 8(a),(b) and (c)).

We can also calculate the most likely number of impacts, $k^\star$, that is, the value of k which maximises $\Phi_{N,p}(k)$ for fixed N and p. Figure 9(a) shows a plot of $k^\star_N(p)$ against p. We do indeed see a very rapid rise in the most likely number of impacts as p increases. Note that $k^\star_N(p)$ is a step function, since the most likely number of impacts is integer valued. Closer investigation of the small p region

suggests a large discontinuity. Figure 9(b) is a plot of the expected number of impacts versus p. Note that the insets expand the small p region in both figures and that $\mu(0) = 0$ in Fig. 9(b). Note that these observations are in qualitative agreement with Figs. 2 and 3. In the next section we shall prove that this sudden jump in $k^\star_N(p)$ does indeed exist.

7 Discontinuity in Most Likely Number of Impacts

We now prove that there is a sudden jump in $k^\star_N(p)$ as a function of p. Since $k^\star$ is the value of k that maximizes $\Phi_{N,p}(k)$, we investigate the difference between two neighbouring points on the curve $\Phi_{N,p}(k)$:

$$\Phi_{N,p}(k+1) - \Phi_{N,p}(k) = \frac{p^k N!}{(N-k)!k(k+1)} \left[-pk^2 + (Np-1)k - 1\right]. \tag{11}$$

Thus $\Phi_{N,p}(k)$ increases or decreases as

$$f_{N,p}(k) = -pk^2 + (Np-1)k - 1 \tag{12}$$

is positive or negative respectively. So any zeros of $f_{N,p}(k)$, given by

$$k_\pm = \frac{1}{2p}\left[(Np-1) \pm \sqrt{(Np-1)^2 - 4p}\right] \tag{13}$$

correspond to turning points of $\Phi_{N,p}(k)$.

We also have that

$$f_{N,p}(0) = -1, \tag{14}$$

$$f_{N,p}(N) = -(N+1). \tag{15}$$

Moreover since

$$f_{N,0}(k) = -(k+1) < 0, \tag{16}$$

and

$$\frac{\partial}{\partial p} f_{N,p}(k) = k(N-k) > 0, \tag{17}$$

for all $k \in (0, N)$, then for fixed N and k, $f_{N,p}(k)$ increases through zero as p increases.

Let us now examine in detail what happens as p increases from zero. At $p = 0$, $f_{N,0}(k)$ is negative for all $k \in (0, N)$ from Eq. (16), thus $\Phi_{N,0}(k)$ is monotone decreasing, and the most likely number of impacting masses is 1.

As p increases, the local (negative) maximum of $f_{N,p}(k)$ at $k = (Np - 1)/2p$ increases until it touches the line $f_{N,p}(k) = 0$. From Eq. (12), this occurs when $(Np - 1)^2 = 4p$, that is when

$$p = p_{\text{crit}} = \left(\frac{1 + \sqrt{N+1}}{N} \right)^2, \tag{18}$$

(Note that the other root corresponds to the unphysical case of $k < 0$). Increasing p still further produces two zeros of $f_{N,p}(k)$ at $k = k_{\pm}$.

Figure 10 shows a sequence of sketches of $f_{N,p}(k)$ and $\Phi_{N,p}(k)$ as p increases from zero. In Fig. 10(a), $p = 0$ and so the most likely number of impacting masses is 1. Increasing p to p_{crit} leads to a repeated root of $f_{N,p}(k)$ (shown in Fig. 10(b)), so $\Phi_{N,p}(k)$ has a stationary inflexion, but is still decreasing, and hence the most likely number of impacts is still 1. Increasing p further, as shown in Fig. 10(c), leads to two zeros of $f_{N,p}(k)$, so $\Phi_{N,p}(k)$ has a local minimum and a local maximum. Initially, the value of $\Phi_{N,p}(k)$ at the local maximum is less than that at $k = 1$, and so the most likely number of impacts is still 1. As p increases still further, there is a critical value at which the local maximum of $\Phi_{N,p}(k)$ becomes a global maximum. At this value of p there is a sudden jump in $k^\star_N(p)$ to a value much larger than 1, as shown in Fig. 10(d). For further increase in p, $k^\star_N(p)$ is monotone increasing, such that $k^\star_N(p) \to N - 1$ as $p \to 1$.

8 A Relation Between σ and p

The numerical simulations in Sec. 2 show a clear jump in the expected number of impacts $k^\star$ as σ is varied. These calculations were performed using the full equations of motion. On the other hand in Sec. 7 we were able to show analytically that an estimate of $k^\star$ also undergoes a sudden jump in value, this time as a function of p. So how can we relate σ and p? In particular, we must find a way to compute p from the parameters in the physical model. We now describe a possible candidate for this relationship.

Solving Eqs. (4) and (5) it is straightforward to show that the separation of masses j and $j + 1$,

$\Delta_j(t) = x_{j+1}(t) - x_j(t)$, is given by

$$\Delta_j(t) = d + (\alpha_{0,j+1} - \alpha_{0,j})\cos\omega t + (\beta_{0,j+1} - \beta_{0,j})\sin\omega t + \frac{\alpha_{1,j+1} - \alpha_{1,j}}{\omega^2 - \Omega^2}\cos\Omega t + \frac{\beta_{1,j+1} - \beta_{1,j}}{\omega^2 - \Omega^2}\sin\Omega t. \quad (19)$$

The quantities $\alpha_{0,j}$ and $\beta_{0,j}$ are related to the initial conditions of the mass j. We assume these are also normally distributed random variables; later we shall integrate over all possible initial conditions.

Now the probability of not having an impact, $1 - p$, is just the probability that $\Delta_j > 0$ for all $t > 0$, that is $P(\inf_{t>0} \Delta_j > 0)$, which gives

$$1 - p = P\left(Y_0 + \frac{Y_1}{|\omega^2 - \Omega^2|} < d\right), \quad (20)$$

where $Y_i, (i = 0, 1)$ is given by

$$Y_i = \sqrt{(\alpha_{i,j+1} - \alpha_{i,j})^2 + (\beta_{i,j+1} - \beta_{i,j})^2}. \quad (21)$$

Equation (20) may be written in terms of the density functions of all the random variables $\alpha_{i,j}$ and $\beta_{i,j}$ with the aid of standard identities from probability theory [Grimmett & Welsh, 1990]. Since $\alpha_{i,j}$ and $\beta_{i,j}$ are normally distributed with zero mean and variance σ^2, then the probability density function of Y_0 is given by

$$f_{Y_0}(x) = \frac{x}{2\sigma^2}\exp\left(-\frac{x^2}{4\sigma^2}\right)H(x), \quad (22)$$

and that for $Y_1/|\omega^2 - \Omega^2|$ by

$$f_{Y_1/|\omega^2-\Omega^2|}(x) = \frac{(\omega^2 - \Omega^2)^2 x}{2\sigma^2}\exp\left(-\frac{(\omega^2 - \Omega^2)^2 x^2}{4\sigma^2}\right)H(x), \quad (23)$$

where $H(x)$ is the Heaviside function. So Eq. (20) becomes

$$1 - p = \int_{-\infty}^{d}\int_{-\infty}^{\infty} f_{Y_0}(t) f_{Y_1/|\omega^2-\Omega^2|}(x - t)\,\mathrm{d}t\,\mathrm{d}x, \quad (24)$$

that is

$$p = 1 - \frac{(\omega^2 - \Omega^2)^2}{4\sigma^4} \int_0^d \int_0^x t(x-t) \exp\left(-\frac{t^2}{4\sigma^2}\right) \exp\left(-\frac{(\omega^2 - \Omega^2)^2 (x-t)^2}{4\sigma^2}\right) \, \mathrm{d}t \, \mathrm{d}x. \qquad (25)$$

We show in Fig. 11 the curve $p = p(\sigma)$ given by Eq. (25) for the parameter values used in the numerical simulation, namely $\omega = 1$, $\Omega_1 = \sqrt{2}$ and $d = 1$.

We are now able to make a quantitative comparison of the predictions of the probabilistic graph theory method and the results of our numerical simulations, with the aid of Eq. (25). Figure 12 shows the expected number of impacts plotted against σ, for both the predictions of the graph theory method and the results of our numerical simulations. We compare the *expected* number of impacts (rather than the most likely number), since this is a much easier statistic to compute reliably in numerical simulations.

Figure 12 shows good qualitative agreement between theory and experiment, particularly for large σ. The value $p(\sigma)$ is extremely small for $\sigma < 0.15$, and we suspect our method of estimating p is poor here. The similarity is encouraging, however, since so many factors were neglected to use the probabilistic graph theory method.

Perhaps the most significant omission is that of the coefficient of restitution at impact. In Sec. 2 our choice of $r = 0.8$ ensured that multiple impacts and sliding were seldom observed. This gave us confidence that we could use graph theory. We choose not to pursue this point further in this paper, and leave calculation of an improved relationship between σ and p for further work. Instead in the next section we shall consider non-simple circuits.

9 Non-simple Circuits

We now consider the possibility of including non-simple circuits in our method. Such a circuit is illustrated in Fig. 6 where 3 impacts are repeated; impact L-1 is repeated twice, impacts 1-2, 3-R repeated once each. First we shall consider those circuits in which exactly one vertex is visited twice, all other vertices being visited no more than once (in other words, just one impact is repeated). Let the number of such circuits of length k in a graph with N vertices be $\phi_N^1(k)$.

Initially let vertex i be visited twice. Then we seek circuits which start at vertex i, visit $\gamma_1 \in \mathbb{N}$

distinct vertices (via a path of length $\gamma_1 + 1$), return to vertex i again, then visit $\gamma_2 \in \mathbb{N}$ more distinct vertices (a path of length $\gamma_2 + 1$), and finally return to vertex i. For a circuit of length k, we have the constraint

$$(\gamma_1 + 1) + (\gamma_2 + 1) = k, \tag{26}$$

and so the number of such circuits is

$$\begin{aligned}
&(N-1)(N-2)\dots(N-\gamma_1)\cdot 1\cdot(N-(\gamma_1+1))(N-(\gamma_1+2))\dots(N-(\gamma_1+\gamma_2)) \\
&= (N-1)(N-2)\dots(N-(\gamma_1+\gamma_2)) && (27)\\
&= (N-1)(N-2)\dots(N-(k-2)) && (28)\\
&= \frac{(N-1)!}{(N-(k-1))!}. && (29)
\end{aligned}$$

Thus the total number of circuits of length k, passing through one vertex twice, and no other vertex more than once is

$$\phi_N^1(k) = \frac{1}{2}\sum\sum_{\substack{\gamma_1,\gamma_2\in\mathbb{N}\\(\gamma_1+1)+(\gamma_2+1)=k}} \frac{(N-1)!}{(N-(k-1))!} = \frac{\gamma(k,2)}{2}\frac{(N-1)!}{(N-(k-1))!}. \tag{30}$$

The factor of $\frac{1}{2}$ arises because each circuit is counted twice. $\gamma(n,j)$ is the number of solutions of the equation

$$\alpha_1 + \alpha_2 + \dots + \alpha_j = n, \tag{31}$$

where $\alpha_i \in \mathbb{N}^+$ for all i and is given [Tucker, 1980] by:

$$\gamma(n,j) = \binom{n-1}{j-1} = \frac{(n-1)!}{(j-1)!(n-j)!}. \tag{32}$$

Thus

$$\phi_N^1(k) = \frac{1}{2}(k-1)\frac{N!}{(N-(k-1))!}. \tag{33}$$

By a similar method, we may count other classes of higher order circuits. We label the number of circuits of length k in a fully connected graph with N vertices where exactly δ_j vertices are visited $j+1$ times, all other vertices visited at most once, as

$$\phi_N^{\dots\delta_4,\delta_3,\delta_2,\delta_1}(k). \tag{34}$$

For example the number of distinct circuits of length $k > 3$ where one vertex is visited three times,

and no other more than once, $\phi_N^{1,0}(k)$, is

$$\phi_N^{1,0}(k) = \frac{1}{6}\frac{(k-1)!}{(k-3)!}\frac{N!}{(N-(k-2))!}. \tag{35}$$

The number of distinct circuits of length $k > 4$ where one vertex is visited four times, and no other more than once, $\phi_N^{1,0,0}(k)$, is

$$\phi_N^{1,0,0}(k) = \frac{1}{24}\frac{(k-1)!}{(k-4)!}\frac{N!}{(N-(k-3))!}. \tag{36}$$

The number of distinct circuits of length $k > 4$ where two vertices are visited twice, and no other more than once, $\phi_N^{2}(k)$, is

$$\phi_N^{2}(k) = \frac{1}{8}\frac{(k-1)!}{(k-4)!}\frac{N!}{(N-(k-2))!}. \tag{37}$$

It is now straightforward to form distribution functions for the number of impacts, extending the sample space to include higher order circuits. Once again we assume impacts occur independently.

To fix ideas let us consider a sample space made up of the five classes of circuit we have counted, that is the simple circuits, and the four higher order circuits above. So the number of circuits with k different mass-mass impacts per period in this case is

$$\phi_N(k) + \phi_N^1(k+1) + \phi_N^{1,0}(k+2) + \phi_N^{1,0,0}(k+3) + \phi_N^2(k+2). \tag{38}$$

Figure 13 shows the distribution of the number of impacts, and their contributions from the five terms of the sum, for various values of p. These diagrams show that, even for very small p, higher order circuits appear to be significant, and as p increases, the higher order circuits dominate, and the probability of observing a simple circuit becomes insignificant, as we would expect. Despite this, however, the shape of each distribution becomes essentially identical as p increases, as shown in Fig. 14, and thus the expectation of the simple circuit distribution alone is a very good approximation to that of the sum. This explains why we have good agreement between theory and numerical simulation for large p; adding higher order circuits does not significantly alter the expected circuit length. For small p, however, the expected circuit length is measurably different, perhaps going some way to account for the poor correspondence in this regime. The behaviour of the most likely circuit length will change also: we expect a sudden jump as before, but at a different critical probability.

Figure 15 shows the change in the expectation of the circuit length, together with our numerical simulations. We do indeed see the most change for small σ, even though the change is modest. It seems more likely that the relationship between p and σ is more important that the inclusion of higher order circuits in determining the agreement between theory and experiment.

10 Conclusions

In this paper we have examined the dynamics of impacts in a large dimensional forced piecewise smooth system. Numerical simulations show a clear jump in the impact statistics as the variance σ^2 of the forcing amplitude is increased.

Initially we assume that the system dynamics consists solely of simple periodic orbits. We count these orbits, using methods from graph theory, and assign to them a certain probability of occurrence. This model also possesses a sudden jump in the expected number of impacts as the impact probability p increases.

A relationship between σ and p is then derived and good agreement is found between the two sets of statistics in the large σ/large p regime. We then refine the model to include multiple impact orbits which slightly improves the agreement in the small σ/small p regime.

There are many possible refinements and improvements to our method, including an explicit inclusion of the coefficient of restitution into our graph theory calculations, allowing non-independence of impacts, or having different values of p for different edges in the graph. Also there are other ways to compute p, for example, by using a more realistic model of mass vibration, and subsequently computing p purely numerically.

Acknowledgements

SJH is extremely grateful to the Centre de Recerca Matematica (CRM), Bellaterra, Catalunya for the facilities to complete part of this work.

References

Biggs, N. L., Lloyd, E. K. & Wilson, R. J. [1976] *Graph Theory 1736–1936* (Clarendon Press, Oxford).

Budd, C. J. & Dux, F. [1994] "Chattering and related behaviour in impact oscillators," *Phil. Trans. Roy. Soc. Lond. A* **347**, 365–389.

Davies, M. A. & Moon, F. C. [1994] "Transition from soliton to chaotic motion during impact of a nonlinear elastic structure," *Chaos Solitons Fractals* **4**, 275–283.

di Bernardo, M., Garofalo, F., Glielmo, L. & Vasca, F. [1998] "Switchings, bifurcations and chaos in DC/DC converters," *IEEE Trans. Circuits Sys. I* **45**, 133–141.

Doole, S. H. & Hogan, S. J. [1996] "A piecewise linear suspension bridge model: nonlinear dynamics and orbit continuation," *Dyn. Stab. Sys.* **11**, 19–29.

Geist, K. & Lauterborn, W. [1988] "The nonlinear dynamics of the damped and driven Toda chain 1. Energy bifurcation diagrams," *Physica D* **31**, 103–116.

Goyder, H. E. D. & Teh, C. E. [1989] "A study of the impact dynamics of loosely supported heat exchanger tubes," *J. Press. Vessel Tech.* **111**, 394–401.

Grimmett, G. R. & Welsh, D. [1990] *Probability: an Introduction* (Clarendon Press, Oxford).

Halse, C., Wilson, R. E., di Bernardo, M. & Homer, M. [2006] "Coexisting solutions and bifurcations in mechanical oscillators with backlash," Submitted.

Hogan, S. J. [1995] "Slender rigid block motion," *ASCE J. Eng. Mech.* **120**, 11–24.

Hogan, S. J. & Homer, M. E. [1999] "Graph theory and piecewise smooth dynamical systems of arbitrary dimension," *Chaos Solitons Fractals* **10**, 1869–1880.

Holmes, P. J. [1982] "The dynamics of repeated impacts with a sinusoidally vibrating table," *J. Sound Vib.* **84**, 173–189.

Homer, M. E. [1999] "Bifurcations and dynamics of piecewise smooth dynamical systems of arbitrary dimension," Ph.D. thesis, University of Bristol.

Kim, S. N. & Jung, S. Y. [2000] "Critical velocity of fluidelastic vibration in a nuclear fuel bundle," *KSME Int. J.* **14**, 816–822.

Kowalczyk, P., di Bernardo, M., Champneys, A. R., Hogan, S. J., Homer, M., Kuznetsov, Y. A., Nordmark, A. B. & Piiroinen, P. T. [2006] "Two-parameter nonsmooth bifurcations of limit cycles: classification and open problems," *Int. J. Bif. Chaos* **16**(3).

Kuroda, M. & Moon, F. C. [2001] "Spatio-temporal dynamics in large arrays of fluid-elastic, Toda-type oscillators," *Phys. Lett. A* **287**, 379–384.

Lazer, A. C. & McKenna, P. J. [1990] "Large-amplitude periodic oscillations in suspension bridges — some new connections with nonlinear-analysis," *SIAM Review* **32**, 537–578.

Rice, S. O. [1945] "Mathematical analysis of random noise," *Bell Sys. Tech. J.* **24**, 46–156.

Stauffer, D. [1985] *Introduction to Percolation Theory* (Taylor & Francis).

Thompson, J. M. T. & Ghaffari, R. [1982] "Chaos after period doubling bifurcations in the resonance of an impact oscillator," *Phys. Lett. A* **91**, 5–8.

Toda, M. [1989] *Theory of Nonlinear Lattices* (Springer, New York), second ed.

Tucker, A. [1980] *Applied Combinatorics* (John Wiley & Sons).

List of Figures

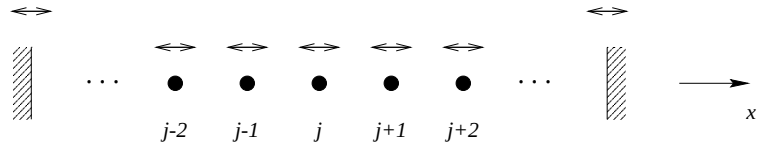

Figure 1: Model configuration

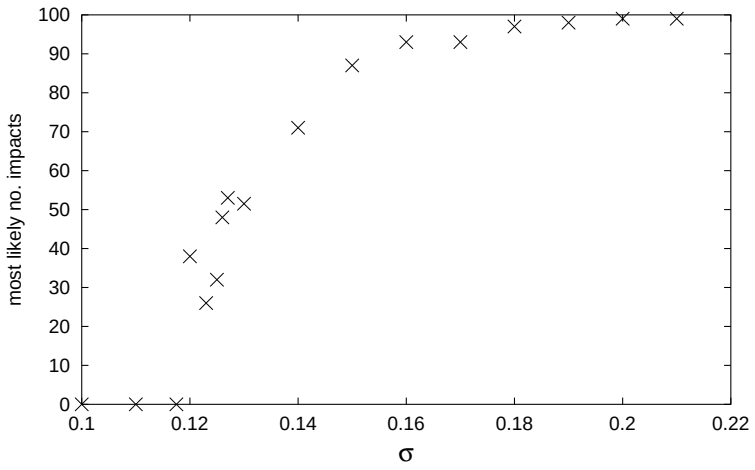

Figure 2: The most likely number of impacts as a function of σ

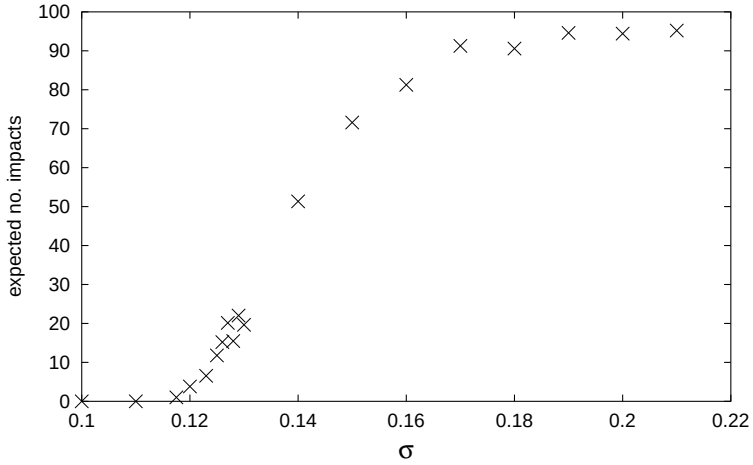

Figure 3: The expected number of impacts as a function of σ

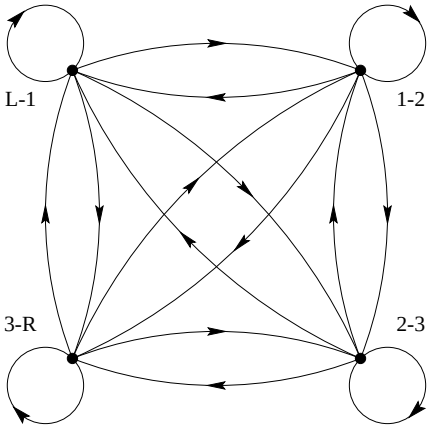

Figure 4: Graph describing periodic motions in the model with $n = 3$ masses. Vertex L-1 denotes an impact between the left hand wall and the first mass, vertex 1-2 an impact between the first and second masses, vertex 2-3 an impact between the second and third masses and vertex 3-R between the third mass and the right hand wall.

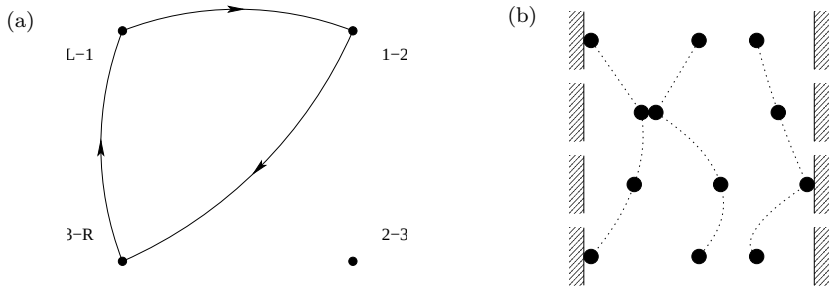

Figure 5: (a) Circuit from Fig. 4, and (b) its physical equivalent.

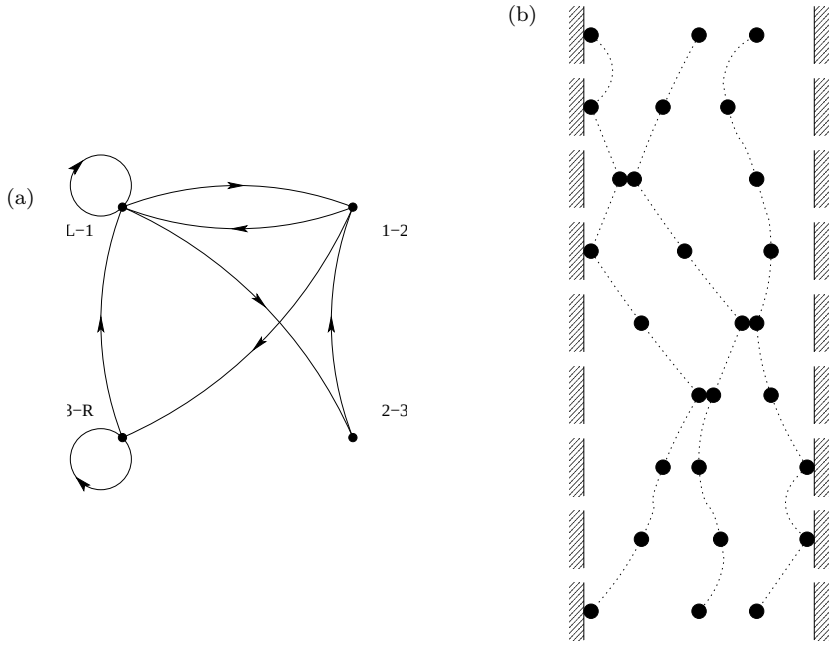

Figure 6: (a) Circuit from Fig. 4, and (b) its physical equivalent.

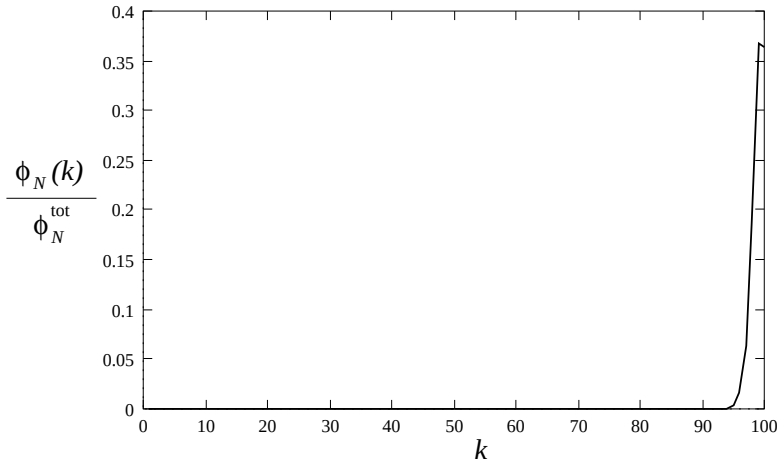

Figure 7: The number of simple circuits of length k for a fully connected graph with $N = 100$ vertices. The ordinate is normalised by the total number of simple circuits, $\phi_N^{\text{tot}} = \sum_{j=1}^{N} \phi_N(j)$

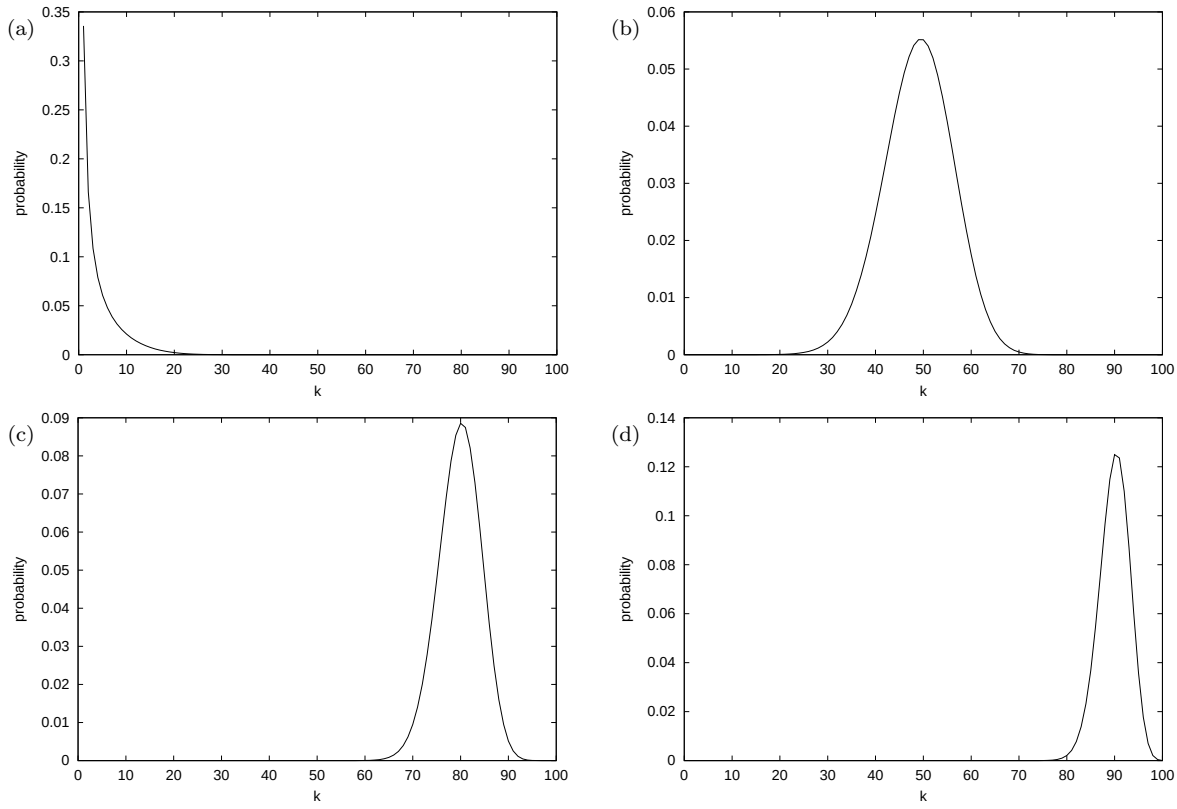

Figure 8: $P(X = k)$ *as a function of* k *with* $N = 100$ *for (a)* $p = 0.01$*, (b)* $p = 0.02$*, (c)* $p = 0.05$ *and (d)* $p = 0.1$*.*

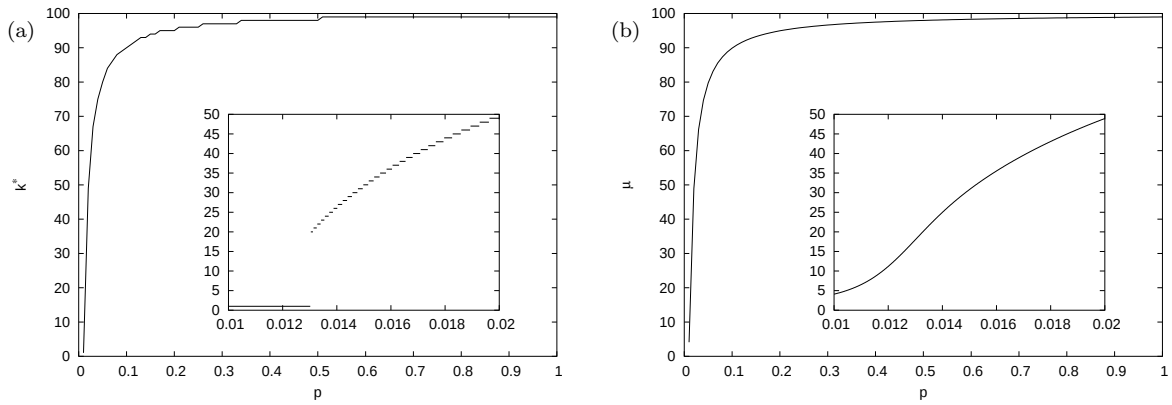

Figure 9: (a) Most likely number ($k^\star$), and (b) expected number (μ) of impacts plotted against p, for $N = 100$, with inserts showing small p region.

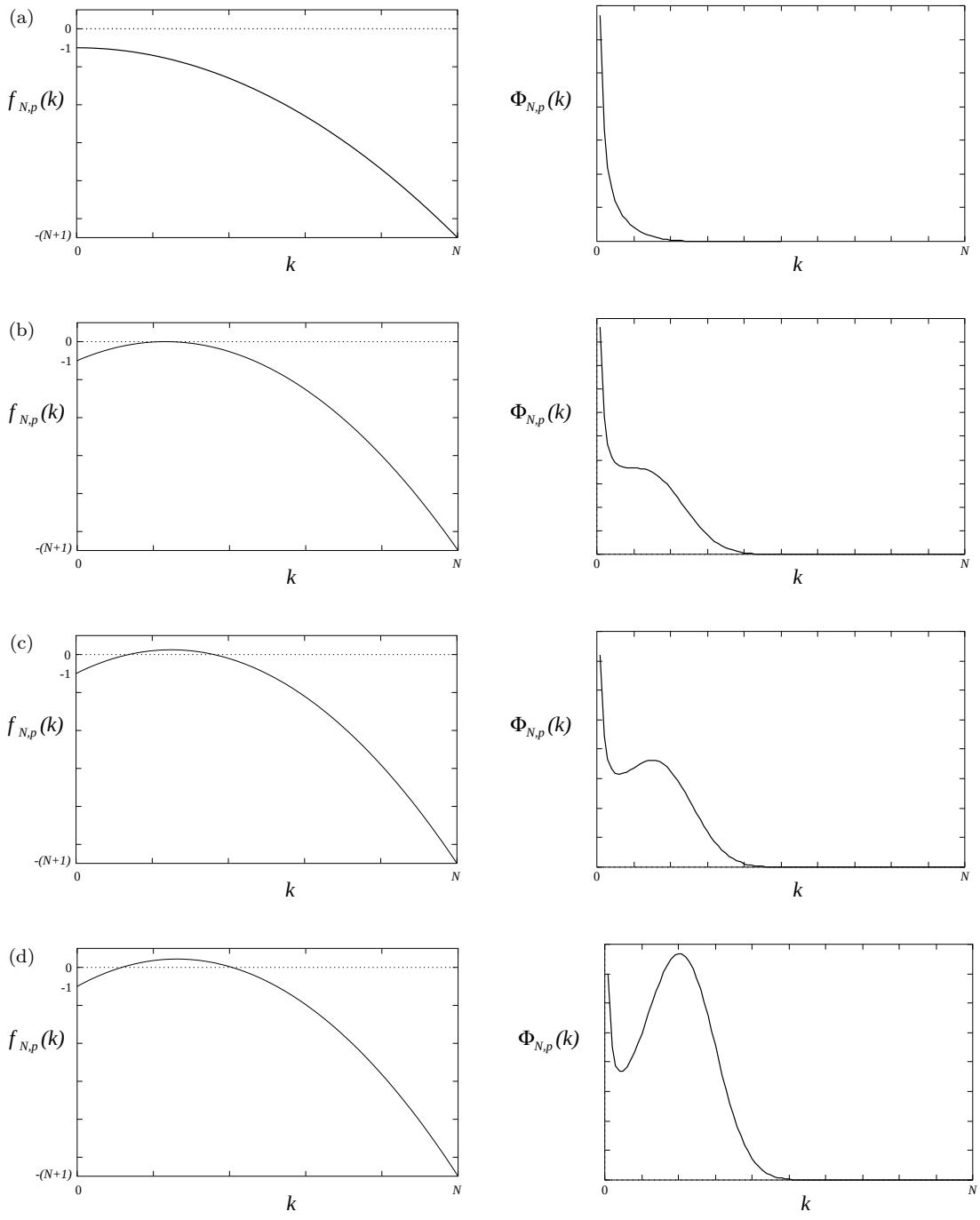

Figure 10: A mechanism for the sudden jump in $k_N^\star(p)$, with impact probability increasing from top to bottom. In a) $p = 0$, in b) $p = p_{\rm crit}$ and in c) and d), $p > p_{\rm crit}$

.

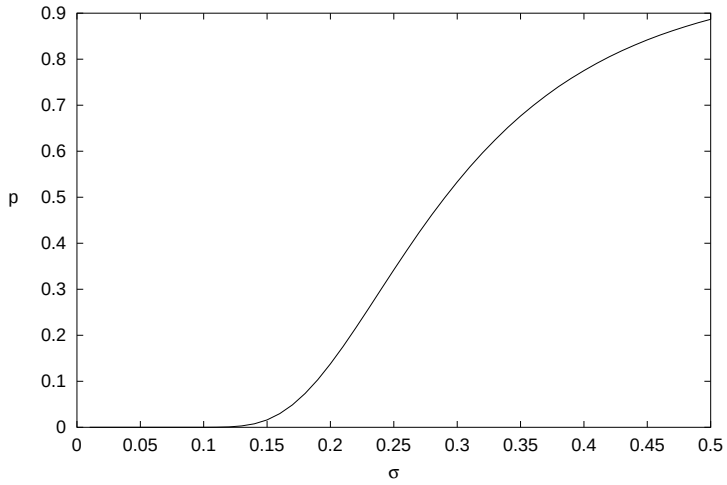

Figure 11: The relationship between impact probability (p) and standard deviation of mass forcing (σ), as given by Eq. (25).

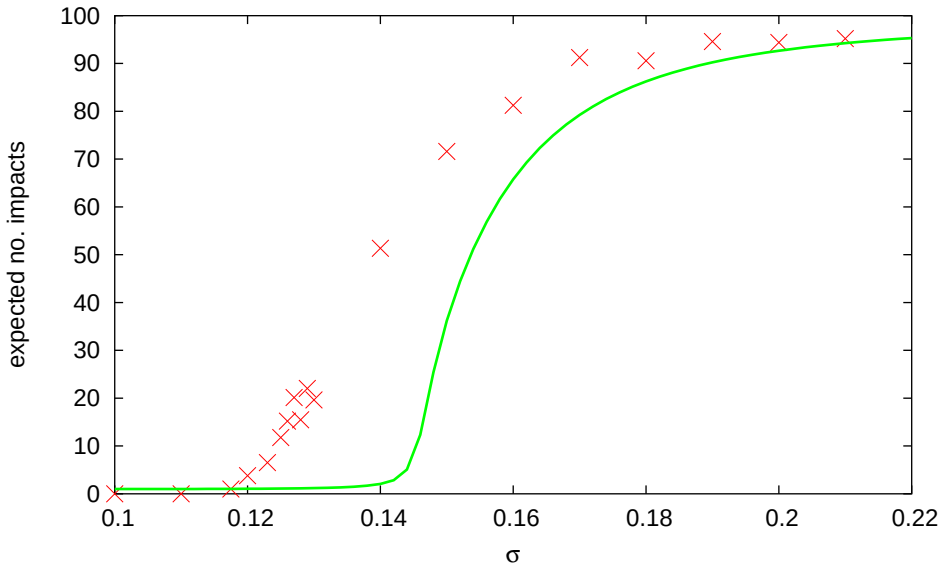

Figure 12: Comparison of expected number of impacts for graph theory predictions (green line) and numerical simulations (red crosses).

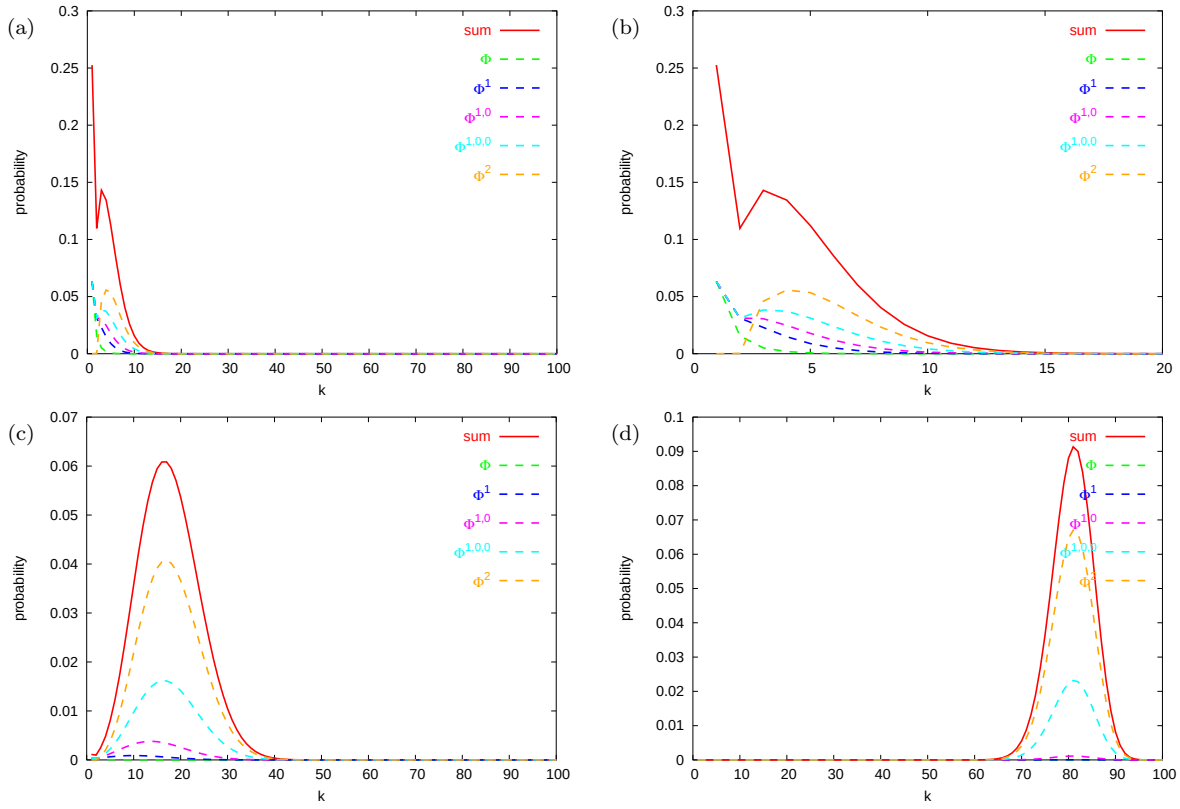

Figure 13: Distributions of the number of impacts (k) with sample space containing higher order circuits (red lines) for $N = 100$, and (a) $p = 0.005$, (b) $p = 0.005$, detail of small k region, (c) $p = 0.01$, (d) $p = 0.05$. Also shown are the relative probabilities of observing the various classes of circuits (dashed lines).

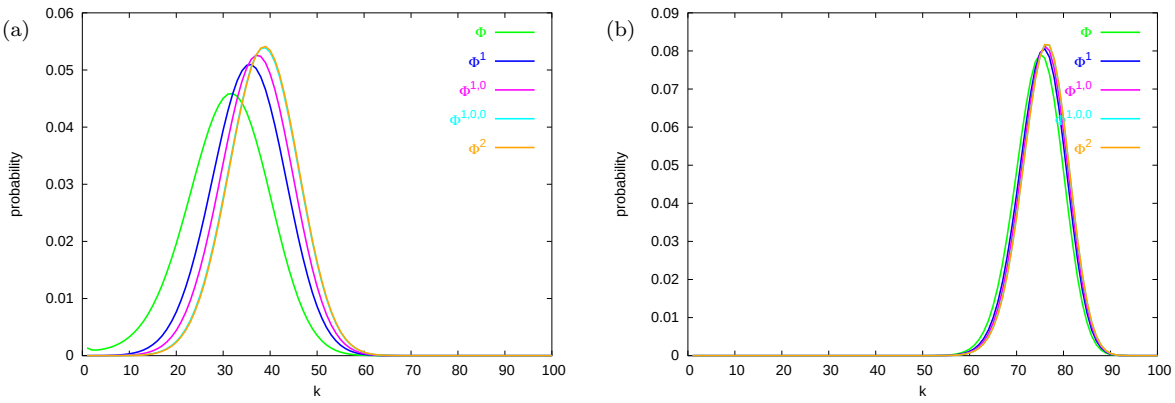

Figure 14: Convergence of simple and higher order circuit distributions as p increases; (a) $p = 0.015$*, (b)* $p = 0.04$*.*

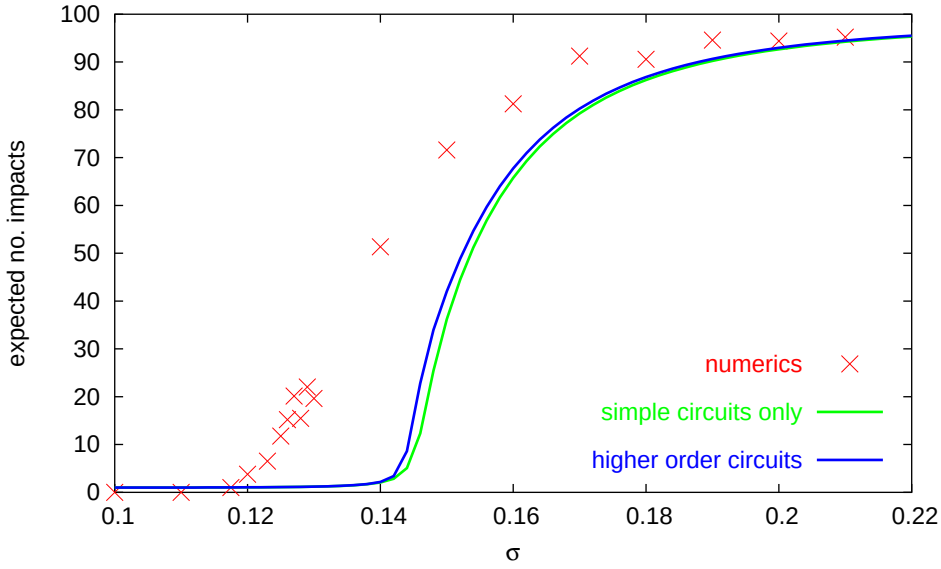

Figure 15: Comparison of expected number of impacting masses for graph theory predictions including higher order circuits (blue line) and simple circuits only (green line), and numerical simulations (red crosses).